IEEE Access
Multidisciplinary | Rapid Review | Open Access Journal

Received July 25, 2020, accepted August 1, 2020, date of publication August 6, 2020, date of current version August 25, 2020.

Digital Object Identifier 10.1109/ACCESS.2020.3014626

Series Active Disturbance Rejection Autopilot Design for Hyper Velocity Projectiles

RUI GONG, RUISHENG SUN, AND WEI CHEN
School of Energy and Power Engineering, Nanjing University of Science and Technology, Nanjing 210094, China

Corresponding author: Ruisheng Sun (rs.sun@njust.edu.cn)

This work was supported in part by the National Natural Science Foundation of China under Grant 51809138, and in part by the China Postdoctoral Science Foundation under Grant 2019M651837.

ABSTRACT This article presents a series active disturbance rejection controller (ADRC) autopilot design scheme with mini pin actuators for nonlinear hyper velocity projectile (HVP) system. In order to accurately describe the flight dynamics of HVP, a new nonlinear model with mismatched disturbances is established considering the aerodynamic characteristics of mini pin actuators. For compensating mismatched disturbances, series ADRC method is incorporated into double-loop (angle loop and angular loop) autopilot design, i.e., in the angle loop mismatched disturbances are observed and compensated in the virtual control calculation; in the angular loop, the observed matched disturbances are compensated in the mini pin control. In addition, both the mismatched and matched disturbances are considered as lumped ones including external disturbances, model uncertainties, coupling terms, etc. Finally, comparative numerical simulations with some traditional nonlinear control methods indicate that the proposed series ADRC HVP system has good robustness performance.

INDEX TERMS HVP, mini pin actuator, attitude autopilot, series ADRC, mismatched disturbances.

I. INTRODUCTION

With the development of new concept weapon such as electromagnetic gun, the muzzle velocity of projectile has already surpassed 7 Mach [1], [2], which provides the technique guarantee for kinetic energy of hyper velocity projectile (HVP). Because of lower cost and great armor-piercing damage ability [3], guided HVP has been chosen as an important part of American next generation ballistic defense system [4]. Usually, HVP flight is with hypersonic velocity, which leads to extremely high dynamic pressure on the projectile and actuator. Consequently, the key problem to control HVP is that traditional high-power actuator cannot be equipped in the projectile with limited space. To solve this technical conundrum, some new concept actuators were presented, such as reaction control system (RCS) [5]–[7], canard rudder [8], [9], and plasma actuator (PA) [10], [11]. However, these actuators have some limitations. RCS uses thrusters arranged around the side direction of projectile to provide attitude control torque as well as translational force. Moreover, due to the discontinuity and limited working time of RCS, it is hard to control HVP flight. Canard rudder has been applied to large-caliber trajectory correction projectile, but the problem of canard wing miniaturization hasn't been solved. The concept of PA is to install one or several plasma discharge at the nose tip to produce the asymmetry of the flow variables around the projectile nose and give an angle of attack to the projectile. Unfortunately, the limitation of battery capacity limits the high-power discharge times of plasma.

As a novel actuator, mini pop-up pin is firstly presented by Georgia Institute of Technology in 2005 [12], [13], which fenced off this question tactfully. By popping up mini pins asymmetrically, HVP can achieve more than 10 gravitational acceleration turn in the effect of high-speed airflow stagnated at pins [14]. After that, a lot of researches on HVP based on mini pins control have been achieved. Silton [15] analyzed mini pins which install near tail wings will generate asymmetric lift on wing to produce roll torque by computational fluid dynamic (CFD) simulation. Massey and Silton [16] presented four different pin geometries to satisfy different maneuverability requirements, and optimized pin deployment schedule for maximum turning authority. Celmins [17] designed and tested a simply electromechanical pin actuator for projectile guidance, with short flight times or limited numbers of

The associate editor coordinating the review of this manuscript and approving it for publication was Halil Ersin Soken.

required actuations. However, these studies only described the effect of mini pins in practice. They did not give a rigorous analysis of dynamic model to consider the influence of mini pins on projectile aerodynamic parameters.

On the basis of aerodynamic data, some simple control laws have been applied to trajectory correction projectile with mini pins. Through approximately linearizing experimental aerodynamic data, Fresconi *et al.* [18] studied the stability of a guided spin-stabilized with mini pins, and found a simple proportional–derivative controller to maneuver the projectile. By Monte Carlo simulation, Fresconi *et al.* [19] proved that the small diameter munition with a rotating pin can afford enough course correction to compensate for ballistic delivery errors. For the same trajectory correction projectile with mini pins, Kai [20] presented a ballistic correction law to make the ballistic drop point close to the target mostly. Unfortunately, these control laws based on trajectory correction projectile with mini pins cannot be applied into the HVP with harsh disturbance and great mobility requirement. Thus, designing an attitude autopilot for HVP with high mobility and strong robustness is necessary.

In addition, the external disturbances and parameter uncertainties exit in attitude dynamic model of HVP on account of harsh flight environment. To improve the robustness of attitude control, Chen *et al.* [21] proposed an adaptive non-singular fixed-time attitude control scheme effectively compensated inertia uncertainties and external disturbances. By using linear active disturbance rejection control (LADRC) technique, Liang *et al.* [22] presented an improved method to actively compensate for the disturbance and improve the attitude system robustness for spacecraft. However, for mismatched disturbances, these methods have certain limitations to completely compensate it. Therefore, many scholars combine the idea of backstepping method with advanced control theory to solve this difficulty, such as adaptive neural network (ANN) [23], echo state network (ESN) [24]. Meanwhile, based on the disturbance observer (DOB) technique such as extend state observer (ESO) [25], [26], Nussbaum disturbance observer (NDO) [27], and sliding mode disturbance observer (SMDO) [28], total disturbances which include mismatched disturbances can be well compensated.

In this article, a new nonlinear mathematic model of HVP is established on the basis of analyzing the aerodynamic parameters change with the introduction of the control pin. The mismatched disturbances caused by control pin and wind exist in the angle loop, which cannot be compensated by feedback linearization (FL) or second-order active disturbance rejection controller (ADRC) method. Therefore, we introduce a virtual control variable and transform conventional ADRC into series form. Then, a double-loop attitude autopilot is designed with great robustness.

The paper is organized as follows. In Section 2, the mathematical model of mini pin control for HVP is deduced, and the characteristics of aerodynamic parameters change with the introduction of the control pin is given. Then, in order to compensate the mismatched disturbances existing in angle loop, series ADRC method is proposed to design attitude autopilot of HVP in Section 3. In Section 4, comparative simulations with some nonlinear control method validate the efficiency of the proposed series ADRC attitude autopilot. Finally, some conclusions are given in Section 5.

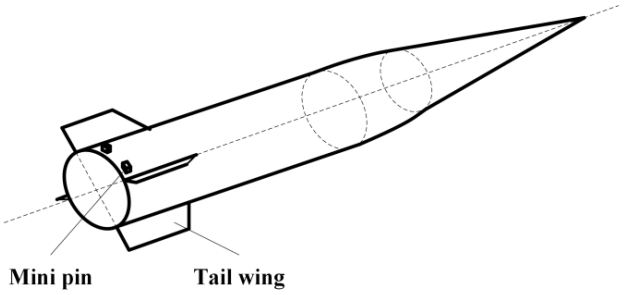

FIGURE 1. Shape of HVP with mini pins.

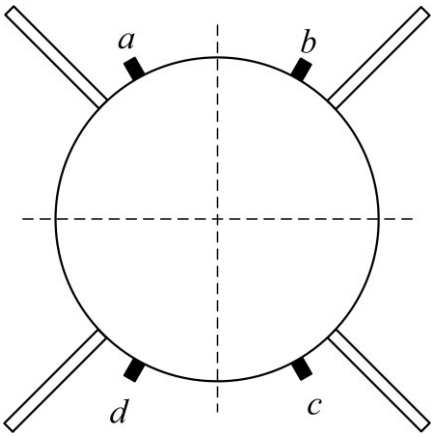

FIGURE 2. The tail view of the HVP.

II. PROBLEM DESCRIPTIONS

A. AERODYNAMIC ANALYSIS FOR MINI PINS

By installing mini pins in the tail of a certain fin-stable projectile, it is inexpensive to convert a conventional projectile into a control projectile [14], as shown in Figure 1.

Specifically, four mini pins which can pop out to a certain height or retract into body are placed near the tail wings, then the attitude of HVP can be controlled by different mini pins configurations. In Figure 2, projectile will generate a positive angle of attack when pin a and b pop out to same height. Similarly, if pop out pin a and d, projectile will generate a sideslip angle. Specially, when pop out pin a and c, the projectile will rotate counterclockwise because the flow field become asymmetrical on both sides of the tail wing caused by mini pin. Therefore, two mini pins with same effect can be configured as a group, and the height of the group is represented by h_x, h_y, and h_z. So we can choose appropriate configuration groups to manage three channels of attitude pitch, yaw and roll, respectively.

To study the influence of mini pins on projectile aerodynamic parameters, CFD simulation and scale model experiment have been carried out on projectile with mini pins by

Kai [20] and Massey *et al.* [12]. The results from analyzing the aerodynamic data are as follows.

Not surprisingly, introduction of the control pin causes aerodynamic parameters change at hyper velocity speeds. Specially, for a given Mach number, axial force coefficient C_{X0}, roll torque coefficient $C_{l\delta}$, and pitching moment coefficient $C_{m_z}^{\alpha}$ pronouncedly increase with the increased pin length. The normal force coefficient C_N^{α} also increases with the introduction of the control pin, but compared with $C_{m_z}^{\alpha}$, the change is much smaller. It indicates that the additional normal force provided by mini pins is much less than the additional pitching moment. Meanwhile, because of different principle from direct aerodynamic parameters, pitch damping moment coefficient $C_{m_z}^{\omega_z}$, and roll damping coefficient $C_{m_x}^{\omega_x}$ nearly do not change with the introduction of the control pins.

Therefore, we use $m_z^{h_z}$ to represent the increased part of $C_{m_z}^{\alpha}$ caused by control pin. The same situation applied to roll torque coefficient $C_{l\delta}$. Because normal force coefficient C_N^{α} is affected by the control pin smaller, so we use $\delta_N^{h_z}$ to represent small increased part.

B. DYNAMICS OF HVP WITH MINI PINS

The mathematical model of the HVP includes the body dynamic model, the aerodynamic model, as well as mini pins model [29]. In order to facilitate discussion, the projectile is treated as a rigid body and its mass is constant. Meanwhile, the influence of gravity is ignored. Thus, the dynamic equations of HVP are

$$\begin{cases} \dot{\alpha} = \omega_z - \omega_x \tan\beta + \omega_y \sin\alpha \tan\beta - \dfrac{N}{mV} \\ \dot{\beta} = \omega_x \sin\alpha + \omega_y + \dfrac{Z}{mV} \\ \dot{\gamma} = \omega_x \\ \dot{\omega}_x = \dfrac{(J_y - J_z)\,\omega_z\omega_y}{J_x} + \dfrac{M_x}{J_x} \\ \dot{\omega}_y = \dfrac{(J_z - J_x)\,\omega_z\omega_x}{J_y} + \dfrac{M_y}{J_y} \\ \dot{\omega}_z = \dfrac{(J_x - J_y)\,\omega_x\omega_y}{J_z} + \dfrac{M_z}{J_z} \end{cases} \tag{1}$$

where the state variables include attack of angle α, sideslip angle β, roll angle γ, roll rate ω_x, yaw rate ω_y, pitch rate ω_z. m is mass of the HVP. J_x, J_y, and J_z are the moments of inertia of three axis, respectively. V means flight velocity. The normal force N, lateral force Z, aerodynamic pitch moment M_x, yaw moment M_y, and pitch moment M_z are all the functions of reference area S, dynamic pressure q, and reference length l as shown in (2).

$$\begin{cases} Ma = \dfrac{V}{\text{Sonic}} \\ N = qS[C_N^{\alpha}(Ma)\alpha + \delta_N^{h_z}(Ma)h_z] \\ Z = qS[C_Z^{\beta}(Ma)\beta + \delta_Z^{h_y}(Ma)h_y] \\ M_x = qSl[m_x^{\omega_x}(Ma)\omega_x + m_x^{h_x}(Ma)h_x] \\ M_y = qSl[m_y^{\omega_y}(Ma)\omega_y + m_y^{\beta}(Ma)\beta + m_y^{h_y}(Ma, h_y)h_y] \\ M_z = qSl[m_z^{\omega_z}(Ma)\omega_z + m_z^{\alpha}(Ma)\alpha + m_z^{h_z}(Ma, h_z)h_z] \end{cases} \tag{2}$$

where Mach number Ma is a function of velocity V and local sonic speed. h_x, h_y, and h_z are the height of pins configuration in three channels, respectively. The aerodynamic coefficients have a nonlinear relationship with Mach number and height of pins.

We assume that the mini pins are ideal actuator without delay, and height of pins is limited within $h_{\max}$. Substituting (2) into (1) and in consideration of $J_y \approx J_z$, then we define the state vectors as $x = \begin{bmatrix}\alpha & \beta & \gamma\end{bmatrix}^T \in \mathbf{R}^{3\times1}$, $\omega = \begin{bmatrix}\omega_x & \omega_y & \omega_z\end{bmatrix}^T \in \mathbf{R}^{3\times1}$, and control vector as $u = \begin{bmatrix}h_x & h_y & h_z\end{bmatrix}^T \in \mathbf{R}^{3\times1}$. The mathematic model of the HVP can be expressed in a strict feedback form as

$$\begin{cases} \dot{x} = \omega + d_x(x, \omega, u, t) \\ \dot{\omega} = g_\omega u + d_\omega(x, \omega, u, t) \end{cases} \tag{3}$$

where the vectors $g_\omega \in \mathbf{R}^{3\times3}$ are:

$$g_\omega = \text{diag}(qS\frac{lm_x^{h_x}}{J_x}, qS\frac{lm_y^{h_y}}{J_y}, qS\frac{lm_z^{h_z}}{J_z}) \tag{4}$$

The disturbances $d_x(x, \omega, u) = \mathbf{R}^{3\times1}$ and $d_\omega(x, \omega, u) = \mathbf{R}^{3\times1}$ in (3) include model uncertainties, channel couplings, and wind disturbances. from equation (1), the elements $\omega_x \tan\beta$, $\omega_y \sin\alpha \tan\beta$, $\omega_x \sin\alpha$, $\left(J_y - J_z\right)\omega_z\omega_y/J_x$, $(J_z - J_x)\,\omega_z\omega_x/J_y$ are the channel couplings. In terms of previous analyzing of aerodynamic, because $\delta_N^{h_z}$ is smaller than $m_z^{h_z}$, the method that indirectly controlling angle through directly controlling angular velocity is appropriate. So N/mV and Z/mV which include $\delta_N^{h_z}$ and $\delta_Z^{h_y}$ respectively are the extra elements of strict feedback form, which can be regarded as disturbances to simplify the controller design. In addition, in consideration of wind disturbances and model uncertainties, we express these effects as disturbances w_α, $w_\beta, w_{\omega_z}, w_{\omega_y}$, which mainly reflect in pitch and yaw channels. In summary, the disturbance d_x and d_ω can be represented as

$$d_x = \begin{bmatrix} -\omega_x \tan\beta + \omega_y \sin\alpha \tan\beta - N/mV + w_\alpha \\ \omega_x \sin\alpha + Z/mV + w_\beta \\ 0 \end{bmatrix} \tag{5}$$

$$d_\omega = \begin{bmatrix} qSlm_x^{\omega_x}\omega_x \\ (J_z - J_x)\,\omega_z\omega_x/J_y + qSl(m_y^{\omega_y}\omega_y + m_y^{\beta}\beta)/J_y + w_{\omega_y} \\ \left(J_x - J_y\right)\omega_x\omega_y/J_z + qSl(m_z^{\omega_z}\omega_z + m_z^{\alpha}\alpha)/J_z + w_{\omega_z} \end{bmatrix} \tag{6}$$

To facilitate the description and calculation of disturbances estimating, we consider the model uncertainties, couplings and wind disturbances as total disturbances. In addition, the disturbance d_x is mismatched and disturbance d_ω is matching.

III. CONTROL DESIGN

A. CONTROL ANALYSIS

According to the system (3), angle loop and angular velocity loop all exist strong disturbances. In order to improve the robustness and adaptability, we choose active disturbance

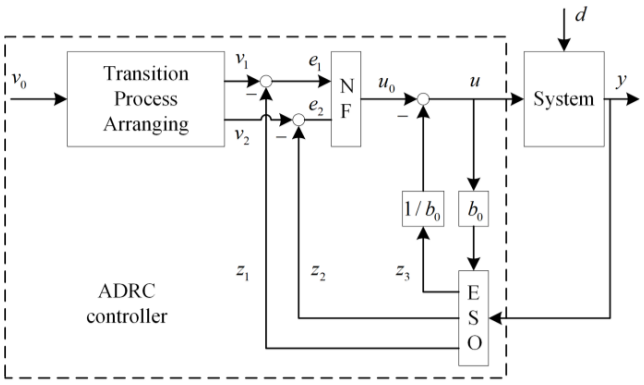

FIGURE 3. ADRC controller structure of the two-order control system.

rejection controller (ADRC) which is independent of an accurate model of system by extended state observer (ESO) to design controller in this article [30], [31].

Meanwhile, by considering the model uncertainties, coupling terms, and wind disturbances as total disturbances, which can be estimated by ESO, the problem of the ''differential expansion'' based on the idea of [32] can be avoided. At the same time, total disturbances estimated by ESO also can easily apply to practical engineering application. For second-order system with common form (7), its standard ADRC controller structure is usually as Figure 3.

$$\begin{cases} \ddot{x} = f(x, \dot{x}, d(t), t) + b(t)u \\ y = x \end{cases} \tag{7}$$

According to Figure 3, ADRC is composed of ''Transition Process Arranging'', ''Nonlinear Feedback (NF)'', and ''Extend State Observer (ESO)''. The role of ''Transition Process Arranging'' is to reduce the impact of initial phase and adjust the overshoot as well as rapidity of system. Meanwhile, unlike linear feedback (LF), NF can improve the dynamic performance of closed loop system. And ESO can extend the disturbance $d(t)$ as state variable z_3, the matching disturbance $f(x, \dot{x}, d(t), t)$ can be compensated well.

But aiming to this nonlinear system (3), especially in the angle loop, mismatched disturbance d_x cannot be compensated by this standard ADRC in Figure 3. Based on the ideal of backstepping method [33], we transform ADRC into series form with the introduction of the virtual control variable, so the mismatched disturbance can be expanded into state by ESO to estimate and compensate. The control system series formation is as shown in Figure 4.

where $v(t)$ is the expected control object. ω' represents virtual control variable for angle state x. d_x, d_ω represent mismatched disturbance and matching disturbance, respectively.

According to Figure 4, because the unknown disturbances d_x exist in the angle loop, the virtual control variable ω' can be generated by the angle loop ADRC to compensated the mismatched disturbances d_x. Then, considering ω' as the expected control object for the angular velocity loop, and angular velocity loop ADRC can give actual control variable to compensate the matching disturbances d_ω and accurately track ω'. Finally, all disturbances can be compensated by series ADRC and track expected control object $v(t)$ well. In addition, compared with backstepping method which need to construct complicated Lyapunov function, series ADRC method just needs simple error feedback and compensating in every step, and the robustness of autopilot designed by series ADRC method is strong which backstepping method cannot achieve.

B. AUTOPILOT DESIGN

In terms of the previous designed series ADRC method, this subsection will propose a control scheme to design autopilot. The discrete algorithm realization of the series ADRC are as follows:

1) TRANSITION PROCESS ARRANGEMENT

The purpose of this part is to reduce the impact of initial phase and solve the contradiction between overshoot and rapidity.

$$v_1 = v_1 - hr_0\, fal(v_1 - v, \alpha_1, h) \tag{8}$$

2) ESO1 OF ADRC1

$$\begin{cases} e_1 = z_{11} - x \\ z_{11} = z_{11} + h(z_{12} - \beta_{11}e_1 + \omega') \\ z_{12} = z_{12} - h\beta_{12}\, fal(e, \alpha_{11}, h) \end{cases} \tag{9}$$

3) VIRTUAL CONTROL VARIABLE OF ADRC1

$$\begin{cases} e_{11} = v_1 - z_{11} \\ \omega_z' = \beta_1\, fal(e_{11}, \alpha_2, \delta_1) - z_{12} \end{cases} \tag{10}$$

4) ESO2 OF ADRC2

$$\begin{cases} e_2 = z_{21} - \omega \\ z_{21} = z_{21} + (z_{22} - \beta_{21}e_2 + b_0u) \\ z_{22} = z_{22} - h\beta_{22}\, fal(e, \alpha_{21}, h) \end{cases} \tag{11}$$

5) SYNTHESIS OF CONTROL VALUE

$$\begin{cases} e_{21} = \omega_z' - z_{21} \\ u = [\beta_2\, fal(e_{21}, \alpha_3, \delta_2) - z_{22}]/b_0 \end{cases} \tag{12}$$

where h is simulation step size. $v \in \mathbf{R}^{3\times1}$ is the control objective. $v_1 \in \mathbf{R}^{3\times1}$ is the optimum track signal of v. And the rise time of control system T_0 is decided by parameter $r_0 \in \mathbf{R}^{3\times3}$. $z_{11} \in \mathbf{R}^{3\times1}$ and $z_{21} \in \mathbf{R}^{3\times1}$ are the estimation of angle state x and angular velocity state ω, respectively. The state variables of ESO $z_{12} \in \mathbf{R}^{3\times1}$ and $z_{22} \in \mathbf{R}^{3\times1}$ are the extended state for mismatched disturbances d_x and matching disturbances d_ω, respectively; $e_1 \in \mathbf{R}^{3\times1}$ and $e_{11} \in \mathbf{R}^{3\times1}$ are the error of estimation and track, respectively; $\beta_{ij} \in \mathbf{R}^{3\times3}$ $(i = 1, 2; j = 1, 2)$ is a positive adjustable parameter. $b_0 \in \mathbf{R}^{3\times3}$ is the estimation of g_ω. fal is a saturation function

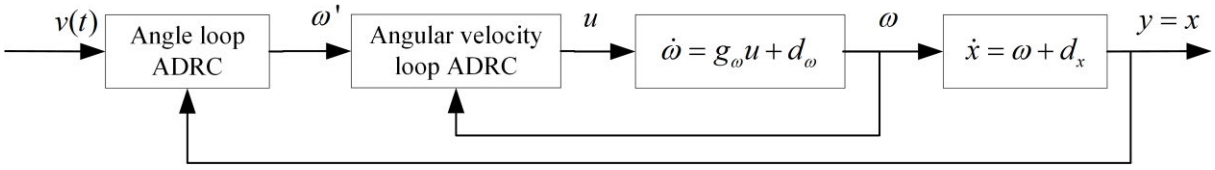

FIGURE 4. Block diagram representation of the series ADRC.

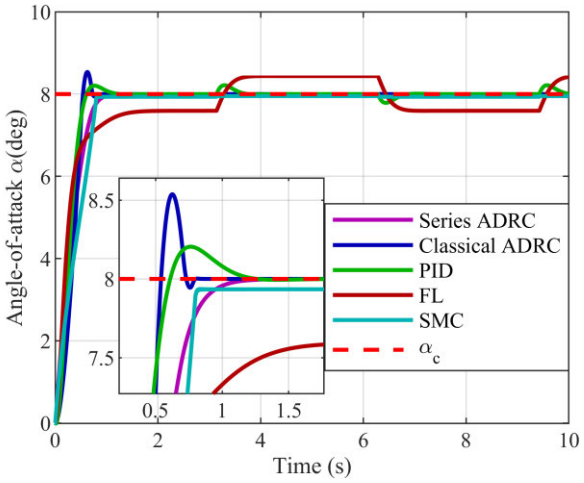

FIGURE 5. The response of the attack angle.

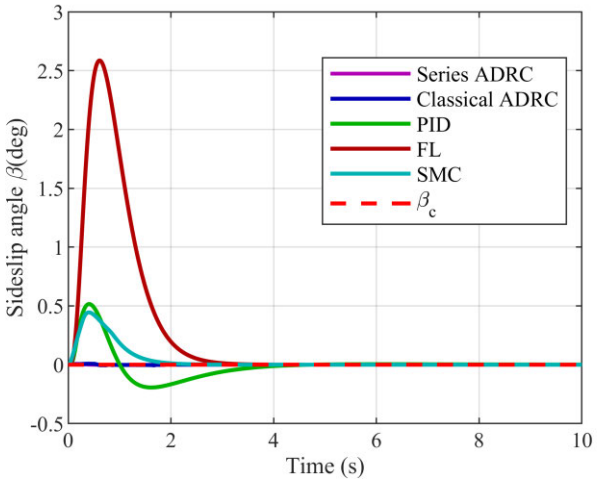

FIGURE 6. The response of the sideslip angle.

which effect is to restrain the signal oscillation, and can be represented as follows:

$$fal(e_i, \sigma_i, \delta) = \begin{cases} e_i/\delta^{1-\sigma_i}, & |e_i| \le \delta \\ |e_i|^{\sigma} \operatorname{sign}(e_i), & |e_i| > \delta \end{cases} \tag{13}$$

Generally, set δ equal to h and σ is an adjustable parameter between 0 and 1.

The convergence and stability analysis for (8) to (12) have been proved in [34].

IV. SIMULATION

In this section, in order to validate the performance of designed attitude control system, an attitude maneuver with large command angles and frequency signal with noise have been considered. The simulation object is a 25mm sub-scale projectile with blunt wing leading and trailing edges, and its mass is 120g and length is 181.4mm. In this simulation, the aerodynamic coefficients are given in [20], [35] while the HVP is flying under 5 Ma. In addition, the dynamics of pins is no more than $|h_{\max}| = 5mm$.

A. TIME RESPONSE ANALYSIS

In order to evaluate the rapidness and accuracy of the series ADRC controller, let the command of angle-of-attack, yaw angle and roll angle are step signal with $\alpha_c = 8°$, $\beta_c = 0°$, and $\gamma_c = 45°$. To verify the robust performance under harsh flight environment, the aerodynamic forces and moment are deflected 20% and the quick wind shear wind(t) = 20sign(sin(t)) is added to pitch channel.

For the method of parameter turning of ADRC, combining with the trial-and-error method, the adjustable parameters of ADRC can be obtained as follows:

$$r_0 = \operatorname{diag}(0.8, 0.8, 4), \quad \alpha_1 = \alpha_2 = \begin{bmatrix} 0.5 & 0.5 & 0.5 \end{bmatrix},$$
$$\alpha_3 = \begin{bmatrix} 1 & 1 & 1 \end{bmatrix}, \quad \alpha_{11} = \alpha_{21} = \begin{bmatrix} 0.5 & 0.5 & 0.5 \end{bmatrix}, \ \delta_1 = \delta_2 = h = 0.001, \quad \beta_{11} = \operatorname{diag}(100, 100, 100), \ \beta_{12} = \beta_{21} = \operatorname{diag}(300, 300, 300), \quad \beta_{22} = \operatorname{diag}(300, 300, 500),$$
$$\beta_1 = \operatorname{diag}(1,50,1), \ \beta_2 = \operatorname{diag}(200,150,1), \ b_0 = 0.9 \cdot g_\omega \text{ kN}.$$

Meanwhile, to ensure that the designed series controller is reasonable and superior, we compare the series ADRC to classical ADRC, feedback linearization (FL) method [36], PID method, and sliding mode control (SMC) method [37]. The comparative simulation was done using MATLAB software and results are presented in Figure 5 to Figure 13.

As shown in Figure 5 to Figure 7, the rise times of these five methods all can achieve 0.9s and 1.7s respectively for angle-of-attack and rolling angle, which indicates its good mobility. The series ADRC method can successfully track the attitude angle commands without overshot under strong disturbance effect. However, because the FL method which is heavily dependent on accurate control model, there is a periodic steady state error in Figure 5 when the wind shear and aerodynamic deflection cause inverse system deviation. Similarly, compared with the PID controller, the control effect

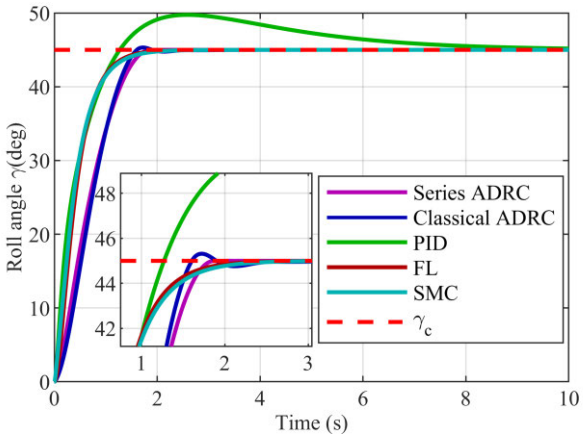

FIGURE 7. The response of the roll angle.

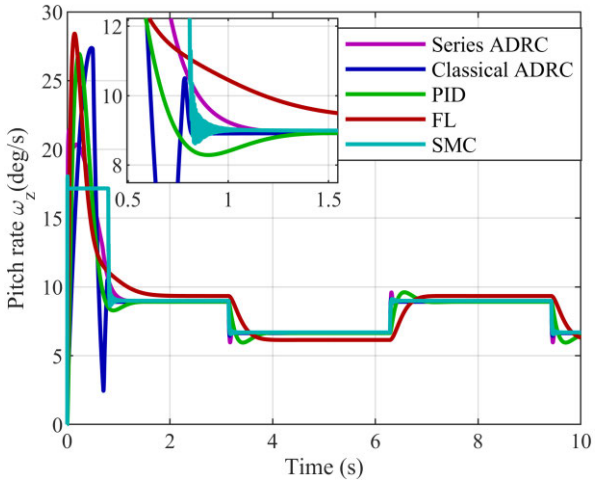

FIGURE 8. The response of the pitch rate.

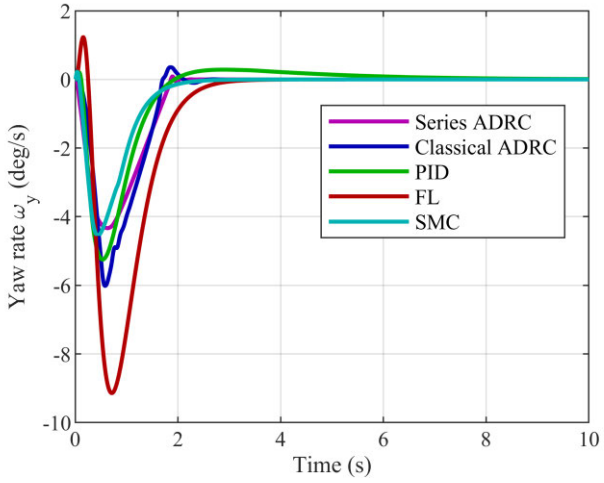

FIGURE 9. The response of the yaw rate.

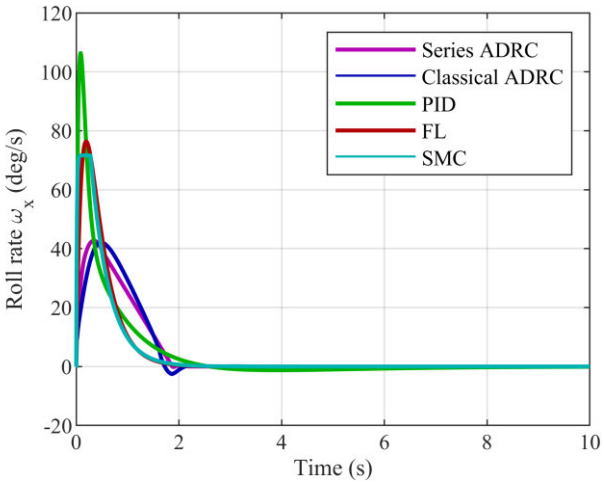

FIGURE 10. The response of the roll rate.

presents a little overshoot due to the disturbance and model uncertainty in Figure 5 and Figure 7. It indicates that the autopilot designed by ADRC method has great robustness in harsh flight environment. Meanwhile, due to the mismatched disturbances, the inevitable overshoot exists in the classical second-order ADRC method. It means that series ADRC can effectively compensate the mismatched disturbances so that robustness of autopilot can be further improved.

From Figure 8 to Figure 10, it is shown that angular rates of three channels rapidly rise to peak and then decline to the same value. Meanwhile, the peak value of the series ADRC is smallest in these five control methods, which means that ADRC can achieve the same result with smaller angle rate which is beneficial to flight stability of HVP. And angle rate can quickly stable to compensate the disturbance, which indicates that ESO can rapidly estimate the disturbance and accurately guide system compensate the disturbance.

In Figure 11 to Figure 13, compared with series ADRC, the SMC method can track the command and compensate the disturbance well by constructing sliding surface, but the chattering phenomenon of control pin occurs obviously, which indicates that the section function *fal* can greatly suppress the chattering phenomenon. Meanwhile, there is impact phenomenon until steady with classical ADRC, which means that ADRC in series form can avoid initial disturbance observation error well caused by mismatched disturbances.

In general, the effect of the series ADRC controller is superior to the other four method. It still has good robustness when the intensive internal and external disturbances exist. The effectiveness of the attitude autopilot designed by series ADRC method satisfies the maneuverability requirement of HVP.

B. FREQUENCY RESPONSE ANALYSIS

In order to validate the frequency performance of designed attitude control system, we replace the command with a sine signal. Meanwhile, take pitch channel as example to facilitate discussion.

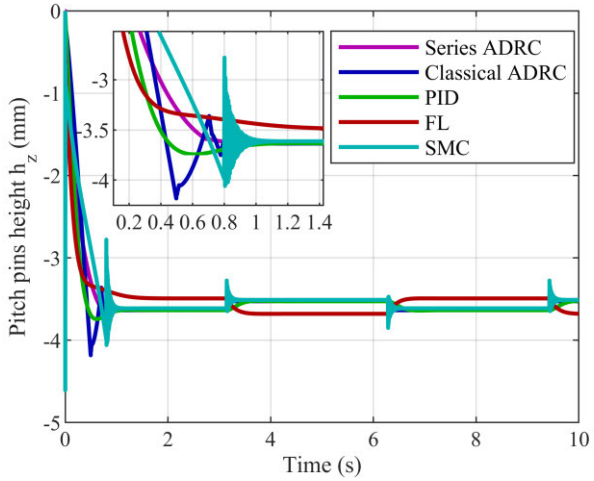

FIGURE 11. The response of the pitch pins height.

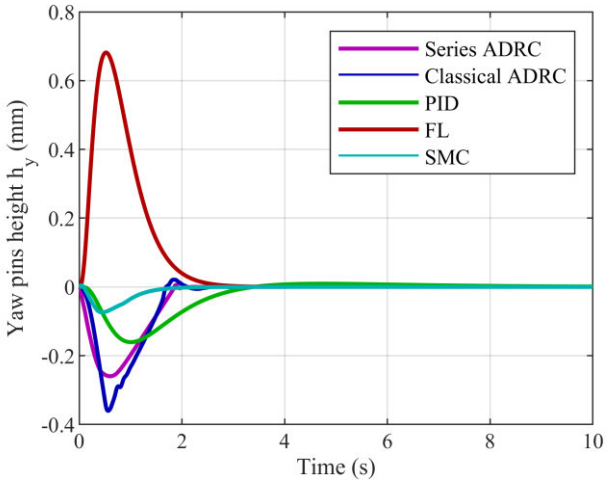

FIGURE 12. The response of the yaw pins height.

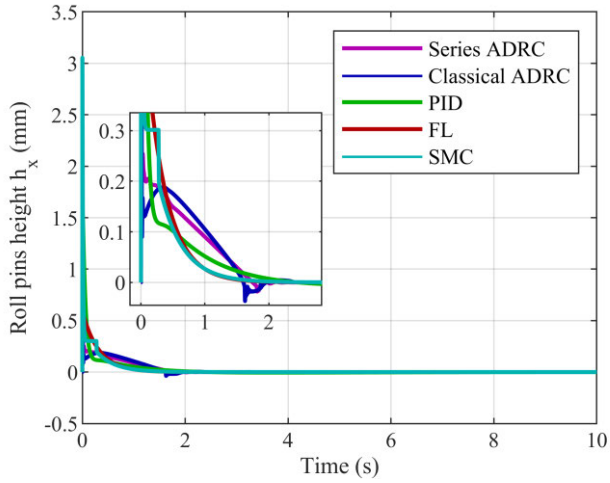

FIGURE 13. The response of the roll pins height.

According to Equation (8) to (12), the rise time of system is mainly decided by transition process arrangement, and specifically decided by adjustable parameter r_0. At the same time, the rise time also has an effect on frequency performance of system. Therefore, in order to analyze the frequency bandwidth characteristics, the autopilot with different parameters r_0 is simulated. Meanwhile, we respectively set command in low (5rad/s), medium (15rad/s), and high (35rad/s) sine frequency to study the change of phase and gain. The results are as presented in Figure 14 to 16.

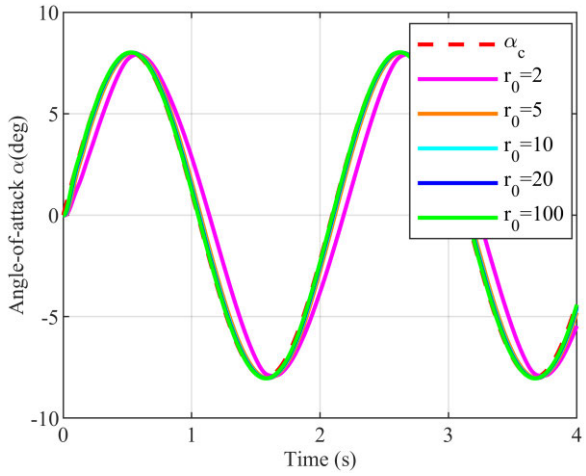

FIGURE 14. The low frequency response of attack angle with different r_0.

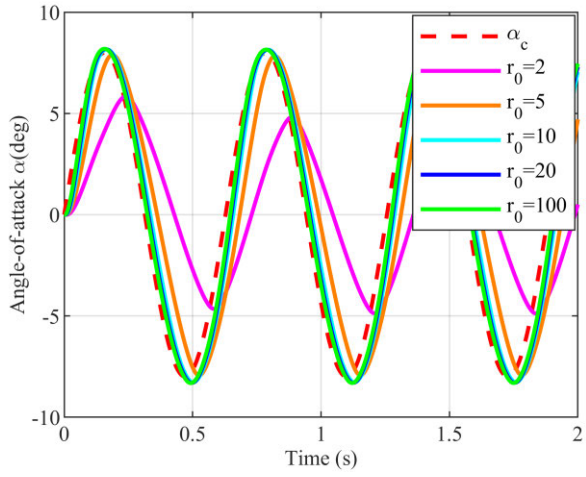

FIGURE 15. The medium frequency response of attack angle with different r_0.

In Figure 14 to 16, the results show that the rise time decreased with the increasing of r_0, phase lag also weakened with r_0 increasing. It indicates that the rapidity of system improves as r_0 enlarge. However, high rapidity will cause autopilot responses to high frequency noise. In addition, it is obvious that amplitude decline exists under high frequency response and also decline with increasing r_0. It means smaller r_0 can restrain high frequency signal better. So we choose $r_0 = 10$ to consider the rapidity and the ability to suppress high frequency noise.

Then, a high frequency noise is added into input command to test the noise reduction ability of autopilot. We set command is $\alpha_c = 8° \sin(15t)$ and noise is $n = 3° \sin(200t)$. The input signal and result are presented in Figure 17.

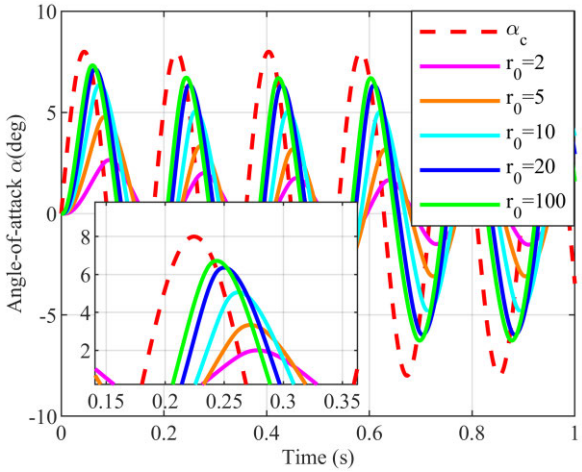

FIGURE 16. The high frequency response of attack angle with different r_0.

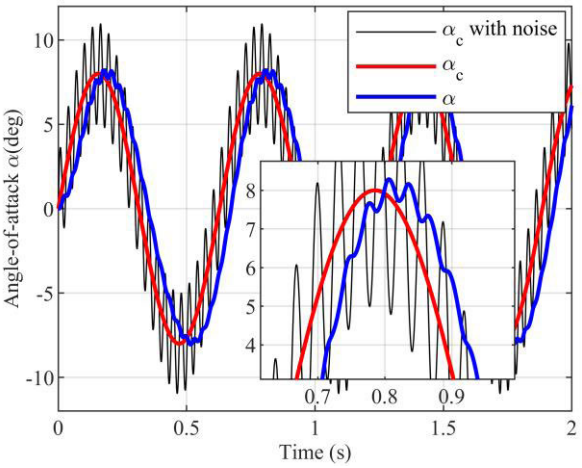

FIGURE 17. The response of attack angle with high frequency noise.

As shown in Figure 17, system is not sensitive to noise. It indicates that the autopilot has good noise reduction ability. At the same time, about 15° phase lag can still meet the requirement of rapidly.

To sum up, by choosing appropriate adjustable parameter r_0, the autopilot can achieve great rapidly and high frequency reduction ability. Meanwhile, the frequency simulation results shown series ADRC method good frequency response stability.

V. CONCLUSION

In this article, based on the HVP's aerodynamic characteristics with the introduction of mini pin actuators, the proposed nonlinear dynamic model can precisely descript the flight of HVP. After that, a double loop (angle loop and angular velocity loop) autopilot for HVP is presented. By introducing a virtual control variable, the series active disturbance rejection controller (ADRC) can guarantee that the autopilot has satisfactory tracking performance and great robustness. The main contribution of the proposed control scheme is to compensate the mismatched disturbances. By using the extended state observer (ESO) to estimate and compensate total disturbances which include external disturbances, model uncertainties, and coupling terms, the autopilot still can normally operate in harsh environment. Finally, the comparative simulation indicates that the effectiveness of the attitude autopilot designed for HVP by series ADRC method can satisfy the mobility and avoid the chattering phenomenon on actuators.

The HVP with mini pins is a complicated nonlinear system, so the new dynamic model possibly cannot accurately describe the flight of HVP. Meanwhile, there are too many parameters and turning difficulties in the design of the series ADRC method. Therefore, how to simplify turning parameters is significance for practical engineering application, this need to be resolved in the future research.

REFERENCES

[1] W. Ma and J. Lu, "Thinking and study of electromagnetic launch technology," *IEEE Trans. Plasma Sci.*, vol. 45, no. 7, pp. 1071–1077, Jul. 2017.
[2] T. Yang, T. Cox, M. Degano, S. Bozhko, and C. Gerada, "History and recent advancements of electric propulsion and integrated electrical power systems for commercial & naval vessels," Univ. Nottingham, Nottingham, U.K., Tech. Rep., 2016.
[3] B. Zohuri, P. McDaniel, J. Lee, and C. J. Rodgers, "New weapon of Tomorrow's battlefield driven by hypersonic velocity," *J. Energy Power Eng.*, vol. 13, no. 5, pp. 177–196, May 2019.
[4] R. O'Rourke, *Navy Lasers, Railgun, and Gun-Launched GuidedProjectile: Background and Issues for Congress*. Washington, DC, USA: Congressional Research Service Washington United States, 2016.
[5] H. Gui, R. Sun, W. Chen, and B. Zhu, "Reaction control system optimization for maneuverable reentry vehicles based on particle swarm optimization," *Discrete Dyn. Nature Soc.*, vol. 2020, pp. 1–11, Mar. 2020.
[6] G. Cai, J. Song, and X. Chen, "Command tracking control system design and evaluation for hypersonic reentry vehicles driven by a reaction control system," *J. Aerosp. Eng.*, vol. 28, no. 4, Jul. 2015, Art. no. 04014115.
[7] R. K. Grandhi and A. Roy, "Effectiveness of a reaction control system jet in a supersonic crossflow," *J. Spacecraft Rockets*, vol. 54, no. 4, pp. 883–891, 2017.
[8] Z. Kaichun, X. Jinwu, and L. Daochun, "Aeroservoelastic modeling and analysis of a canard-configured air-breathing hypersonic vehicles," *Chin. J. Aeronaut.*, vol. 26, no. 4, pp. 831–840, Aug. 2013.
[9] X. L. Ji, H. P. Wang, S. M. Zeng, and C. Y. Jia, "Lateral-directional aerodynamics of a canard guided spin stabilized projectile at supersonic velocity," *Appl. Mech. Mater.*, vols. 110–116, pp. 4343–4350, Oct. 2011.
[10] P. Gnemmi, R. Charon, J.-P. Dupéroux, and A. George, "Feasibility study for steering a supersonic projectile by a plasma actuator," *AIAA J.*, vol. 46, no. 6, pp. 1308–1317, Jun. 2008.
[11] P. Gnemmi and C. Rey, "Plasma actuation for the control of a supersonic projectile," *J. Spacecraft Rockets*, vol. 46, no. 5, pp. 989–998, Sep. 2009.
[12] K. C. Massey, J. Mcmichael, T. Warnock, and F. Hay, "Mechanical actuators for guidance of a supersonic projectile," *J. Spacecraft Rockets*, vol. 45, no. 4, pp. 802–812, Jul. 2008.
[13] K. C. Massey, J. Mcmichael, T. Warnock, and F. Hay, "Design and wind tunnel testing of guidance pins for supersonic projectiles," in *Proc. Transformational Sci. Technol. Current Future Force*, Nov. 2006, pp. 121–128.
[14] K. Massey, K. Guthrie, and S. Silton, "Optimized guidance of a supersonic projectile using pin based actuators," in *Proc. 23rd AIAA Appl. Aerodyn. Conf.*, Jun. 2005, p. 4966.
[15] S. Silton, "Comparison of predicted actuator performance for guidance of supersonic projectiles to measured range data," in *Proc. 22nd Appl. Aerodyn. Conf. Exhib*, Aug. 2004, p. 5195.
[16] K. Massey and S. Silton, "Testing the maneuvering performance of a mach 4 projectile," in *Proc. 24th AIAA Appl. Aerodyn. Conf.*, Jun. 2006, p. 3649.
[17] I. Celmins, "Design and evaluation of an electromechanical actuator for projectile guidance," Army Res. Lab., Adelphi, MD, USA, Tech. Rep. ARL-MR-0627, 2007.

[18] F. Fresconi, G. Cooper, I. Celmins, J. DeSpirito, and M. Costello, "Flight mechanics of a novel guided spin-stabilized projectile concept," *Proc. Inst. Mech. Eng., G, J. Aerosp. Eng.*, vol. 226, no. 3, pp. 327–340, Mar. 2012.
[19] F. Fresconi, J. DeSpirito, and I. Celmins, "Flight performance of a small diameter munition with a rotating wing actuator," *J. Spacecraft Rockets*, vol. 52, no. 2, pp. 305–319, Mar. 2015.
[20] L. Kai, *Aerodynamic Ballistic Characteristics of Ballistic Correction Projectile Based on Miniature Spoiler*. Nanjing, China: Nanjing Univ. Science & Technology, 2018.
[21] Q. Chen, S. Xie, M. Sun, and X. He, "Adaptive nonsingular fixed-time attitude stabilization of uncertain spacecraft," *IEEE Trans. Aerosp. Electron. Syst.*, vol. 54, no. 6, pp. 2937–2950, Dec. 2018.
[22] L. Yu, R. Wang, T. Liu, and W. Wang, "Attitude control for spacecraft based on linear active disturbance rejection control technique," in *Proc. IEEE Int. Conf. Inf. Autom.*, Aug. 2015, pp. 3084–3088.
[23] X. Cao, P. Shi, Z. Li, and M. Liu, "Neural-network-based adaptive backstepping control with application to spacecraft attitude regulation," *IEEE Trans. Neural Netw. Learn. Syst.*, vol. 29, no. 9, pp. 4303–4313, Sep. 2018.
[24] Q. Chen, H. Shi, and M. Sun, "Echo state network-based backstepping adaptive iterative learning control for strict-feedback systems: An error-tracking approach," *IEEE Trans. Cybern.*, vol. 50, no. 7, pp. 3009–3022, Jul. 2020.
[25] S. Zhang, Q. Wang, G. Yang, and M. Zhang, "Anti-disturbance backstepping control for air-breathing hypersonic vehicles based on extended state observer," *ISA Trans.*, vol. 92, pp. 84–93, Sep. 2019.
[26] B. Ning, S. Cheng, and Y. Qin, "Direct torque control of PMSM using sliding mode backstepping control with extended state observer," *J. Vibrat. Control*, vol. 24, no. 4, pp. 694–707, Feb. 2018.
[27] C. Wang, J. Jiang, X. Wu, and L. Wu, "Switching motion control of aircraft skin inspection robot using backstepping scheme and nussbaum disturbance observer," *Int. J. Control, Autom. Syst.*, vol. 16, no. 6, pp. 2948–2957, Dec. 2018.
[28] J. Sun, J. Yi, Z. Pu, and X. Tan, "Fixed-time sliding mode disturbance observer-based nonsmooth backstepping control for hypersonic vehicles," *IEEE Trans. Syst., Man, Cybern. Syst.*, early access, Jul. 2, 2018, doi: 10.1109/TSMC.2018.2847706.
[29] Z. Yaxing, *Reseacch on Attitude Control for Missile With Blended Lateral Thrust and Aerodynamic Force*. Harbin, China: Harbin Institute of Technology, 2016.
[30] J. Han, "Auto-disturbances-rejection Controller and Its Applications," *Control Decis.*, vol. 13, no. 1, pp. 19–23, 1998.
[31] C. QinN Qi and K. Zhu, "Active disturbance rejection attitude control design for hypersonic vehicle," *Syst. Eng. Electron.*, vol. 33, no. 7, pp. 1607–1610, 2011.
[32] C. Sheng, *Investigation on Hardware-in-the-Loop Simulation Algorithm of Diving Guidance Technology for Hypersonic Vehicle*. Changsha, China: National Univ. Defence Technology, 2015.
[33] Y. Bai, Y. Cao, and T. Li, "Optimized backstepping design for ship course following control based on actor-critic architecture with input saturation," *IEEE Access*, vol. 7, pp. 73516–73528, 2019.
[34] Z. H. Wu and B. Z. Guo, "On convergence of active disturbance rejection control for a class of uncertain stochastic nonlinear Systems," *Int. J. Control*, vol. 92, no. 5, pp. 1103–1116, 2017.
[35] H. Yucai, *Aerodynamic Analysis and Ballistic Simulation about Hypersonic Projectile*. Nanjing, China: Nanjing Univ. Science Technology, 2017.
[36] J. Dong, D. Zhou, C. Shao, and S. Wu, "Nonlinear system controllability analysis and autopilot design for bank-to-turn aircraft with two flaps," *Proc. Inst. Mech. Eng., G, J. Aerosp. Eng.*, vol. 233, no. 5, pp. 1772–1783, Apr. 2019.
[37] Y. Zhang and P. Yan, "An adaptive integral sliding mode control approach for piezoelectric nano-manipulation with optimal transient performance," *Mechatronics*, vol. 52, pp. 119–126, Jun. 2018.

RUI GONG received the B.S. degree from the Nanjing University of Science and Technology, Nanjing, China, in 2019, where he is currently pursuing the master's degree. His main research interests include guidance and control application.

RUISHENG SUN received the Ph.D. degree in navigation, guidance and control from the Nanjing University of Science and Technology (NJUST), Nanjing, China, in 2010. He is currently a Professor and a Ph.D. Supervisor with NJUST. His research interests include nonlinear adaptive control and guidance, adaptive observer design, and multidiscipline optimization.

WEI CHEN received the B.S., M.E., and Ph.D. degrees from Northwestern Polytechnical University, Xi'an, China, in 2010, 2013, and 2017, respectively. He is currently a Lecturer with the Nanjing University of Science and Technology (NJUST), Nanjing, China. His research interests include cooperative navigation and localization for underwater vehicles, simultaneous input and state estimation, and moving horizon estimation.